INFLUENCE OF MAGNETIC FIELD ON GAS BUBBLES FLOW IN LIQUID METAL

S. Pavlovs[(1)], A. Jakovics[(1)], E. Baake[(2)], V. Sushkovs[(1)]

[(1)]Laboratory for Mathematical Modelling of Environmental and Technological Processes, University of Latvia, 25 Zellu str., LV-1002, Riga, Latvia
[(2)]Institute of Electrotechnology, Leibniz University of Hannover, Wilhelm-Busch-Str. 4, D-30167 Hannover, Germany

ABSTRACT. The paper presents the results of numerical computations of gas bubbles flow through electrically conductive liquid in external uniform magnetic field.

Euler-Euler approach, realized with *Magnetohydrodynamic (MHD) module* of *ANSYS Fluent* commercial package, is used for multiphase flow: continuous phase is electrically conductive liquid and dispersed phase is gas bubbles.

Transient distributions of physical fields, computed with *LES* (*Large Eddy Simulation*) for gas turbulent flow through electrically conductive liquid, influenced with magnetic field, are discussed. Computed profiles of liquid velocity are compared with experimentally measured profiles for air–water and nitrogen–*Wood*-metal *cylindrical bubble reactor* (*CBR*).

INTRODUCTION

The production of hydrogen H_2 without generation of carbonic acid CO_2 may be performed with decomposition of methane $CH_4 \rightarrow C+2H_2$. The reasonable rate of this endothermic reaction ($\Delta h_0 = 74.85\ kJ/mol$) is reached at temperature values above 600^oC [1]. The main problem of such process is the decreasing of reactor life. The cause is deposition of carbon particles on the reactor walls and catalyst surface, as the consequence is the pressure drop and increase of thermal resistance.

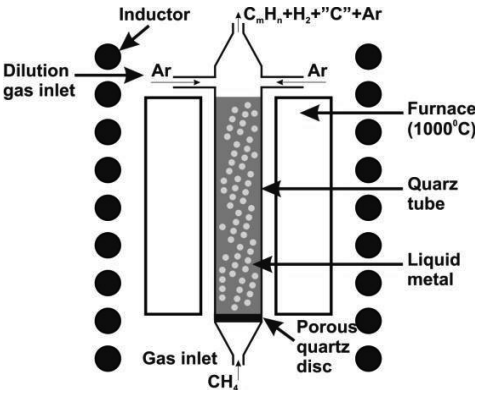

Figure 1. Liquid metal bubble column for H_2 production without CO_2 emission

A possible way to increase efficiency of production and to control the process is the utilization of magnetic field, produced by *direct current* (*DC*) or *alternating current* (*AC*) source, acting on electrically conductive liquid, when methane bubbles are flowing through it. The mentioned above process is realized with methane–tin *CBR* [2], the scheme of installation is shown in Figure 1 [3].

Previous consideration of single bubble dynamics [4] and bubbles collective dynamics [5] are continued in current paper with in-depth analysis of gas bubbles flow through electrically conductive liquid in uniform external magnetic field.

Experimental verification of numerical model with available measurement data without magnetic field have been performed as well.

MULTIPHASE *EULER-EULER* APPROACH

The system of hydrodynamic equations for two-phase system of gas and liquid (all values have upper or lower index "*g*" and "*l*" accordingly) consist of continuity, volume conservation and momentum equations according to *Euler-Euler* approach, which is realized in commercial packages – *ANSYS CFX* [6] and *ANSYS Fluent* [7].

The closure of equation system is performed with constrain on the pressure, namely two phases share the same pressure field. Static pressure in liquid depends on height z from the reactor bottom [8]:

$$p = p_{op} + g_0 \rho_l (H_R - z) \tag{1}$$

where p_{op} is the operating pressure, g_0 is gravitational acceleration, H_R is reactor height.

The gas density ρ_g is derived from ideal gas law

$$\rho_g = \frac{pM_g}{R_0 T} \tag{2}$$

where $R_0 = 8.314 \cdot 10^3 \, kJ/(kmol \cdot K)$ is the universal gas constant, M_g is the molar mass of gas phase.

The flow is assumed to be isothermal, thus temperature is equal to operation temperature $T = T_{op}$. The liquid density is uniform constant.

In momentum equations only ***buoyancy*** force and ***drag*** force may be taken into account from the set of interfacial forces, acting on one phase due to the presence of other phase [6,7]. The computations during the tuning of numerical model show that the changes of distribution of gas volume fraction due to other forces' contribution (including ***lift*** force, ***virtual mass*** force and ***wall lubrication*** force) does not exceeded 5%. The ***interphase turbulent dispersion*** force is not applicable for *LES* model of turbulence. This force may be used only with models of homogeneous turbulence such as *k-ω Shear Stress Transport* (*SST*) model.

ELECTROMAGNETIC FORCE

The electromagnetic (EM) force $\vec{f}_l^{EM}$, which acts in electrically conductive liquid flowing in external uniform magnetic field $\vec{B}_0$, is the following

$$\vec{f}_l^{EM} = \vec{j}_l \times \vec{B}_0 \tag{3}$$

There are two approaches for computation of electrical current $\vec{j}_l$, induced in electrically conductive liquid, flowing with velocity $\vec{v}_l$ in external magnetic field $\vec{B}_0$.

It is assumed that magnetic field $\vec{B}_{ind}$ of induced electrical current is extremely small in comparison with external magnetic field $\vec{B}_0$

$$\vec{B}_{ind} << \vec{B}_0 \tag{4}$$

Equation for electrical potential. For taking into account the closure of lines ($div\ \vec{j}_l = 0$) of electrical current $\vec{j}_l = \phi_l \sigma_l^{EM} \left(-\nabla\varphi + \vec{v}_l \times \vec{B} \right)$, which is determined with *Ohm*'s law, the equation for electrical potential φ is formulated as follows

$$div\left(\phi_l \sigma_l^{EM} grad\varphi\right) = div\left(\phi_l \sigma_l^{EM}\, \vec{v}_l \times \vec{B}\right) \tag{5}$$

where volume fraction of liquid is ϕ_l and its electrical conductivity is σ_l^{EM}.

The boundary conditions for electrical potential at electrically non-conductive walls are *Neumann* type conditions

$$\left.\frac{\partial\varphi}{\partial n}\right|_{S_{non-cond}} = 0 \tag{6}$$

Equations for magnetic induction. Induced electrical current density $\vec{j}_l$ for Eq. 3 can be determined with *Ampere's* law

$$\vec{j}_l = \frac{1}{\mu_0} rot\ \vec{B}_{ind} \tag{7}$$

where $\mu_0 = 4\pi \cdot 10^{-7}\ H/m$ is magnetic constant.

The distribution of induction $\vec{B}_{ind}$ of magnetic field of electrical current, induced by flow of electrically conductive liquid in external magnetic field, can be found from equation, which derived using *Ampere's*, *Faraday's* and *Ohm's* laws, and then can be rewritten in the classic form of transport equation

$$\frac{\partial \vec{B}_{ind}}{\partial t} + (\vec{v}_l \cdot \nabla)\vec{B}_{ind} = \frac{1}{\mu_0 \phi_l \sigma_l^{EM}} \Delta \vec{B}_{ind} - \frac{1}{\mu_0} grad\left(\frac{1}{\phi_l \sigma_l^{EM}}\right) \times rot\ \vec{B}_{ind} + \left[\left(\vec{B}_0 + \vec{B}_{ind}\right) \cdot \nabla\right] \vec{v}_l \tag{8}$$

The boundary conditions for $\vec{B}_{ind}$ at electrically non-conductive walls are *Dirichlet* type conditions for both normal (n) and tangential (τ) components

$$\left.\vec{B}_{ind}\right|_{S_{non-cond}} = \left.\{B_{ind,n}; B_{ind,\tau}\}\right|_{S_{non-cond}} = 0 \tag{9}$$

Pros and cons of potential and induction methods.

• Electrical potential method needs the solution of a single scalar equation, but with *Neumann* type boundary conditions in case of electrically insulated walls. It's means, that it's necessary to specify artificially the potential value in a single arbitrary point. The solution of such a problem has a risk of instability of numerical procedure.

• Magnetic induction method needs the solution of three scalar equations (for all components of magnetic induction vector), but with *Dirichlet* type boundary conditions for both electrically insulated and conductive walls. Numerical procedure for such a problem is more stable in comparison with similar procedure for problem with *Neumann* type conditions.

PECULIARITIES OF NUMERICAL COMPUTATIONS

Sequence of computations. As the distribution of electrical conductivity of liquid depends on its volume fractions the computations of EM field must be performed simultaneously with hydrodynamics problem solution. The sequence of the further computations depends on choice of package, which performs the hydrodynamics computations.

• If *ANSYS CFX* package is chosen [6,9] the computations using Eq. 5 and boundary conditions Eq. 6 or Eq. 8 and boundary conditions Eq. 9 need the application of *ANSYS EMAG* module of *ANSYS Multiphysics* package. The both mentioned packages need consequent application until the desired computations precision is reached.

• In case of choice of *ANSYS Fluent* package [7,10] the special *ANSYS Fluent MHD Module* is needed [11], which realizes the computations according to electrical potential formulation or according to magnetic induction formulation simultaneously with solution of hydrodynamics problem for gas-liquid two-phase system.

For the further computations *ANSYS Fluent MHD Module* has been chosen.

Mesh and time step. The numerical study of the gas-liquid flow have been performed using the structured 3D mesh (~550–950 hundreds of elements) with the inflation in the horizontal and vertical directions from the inlet zone to the walls and to the outlet zone.

To ensure the stability of computations for the transient flow regime the time step is chosen in the range 0.001–0.005 *sec*, which corresponds to the *Courant* number value less then the unity. When flow changes in time are extremely fast (after the start of gas injection into liquid volume or in case of "switching on" of magnetic field), to gain the stability of computations the time step has been chosen extremely small – up to 0.0001–0.00005 *sec*.

VERIFICATION OF COMPUTATIONAL MODEL

Computational results have been compared with experimental data for the following geometries and two-phase system properties:

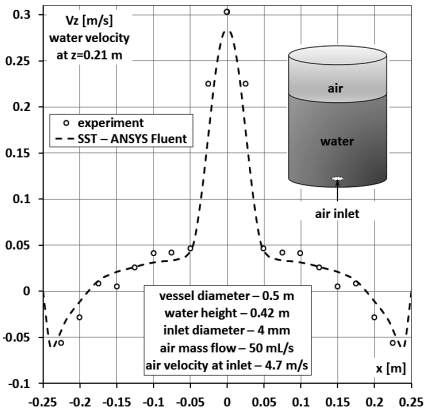

Figure 2. Water velocity vertical component for air–water *CBR*. Comparison of experimental data [8] and computational results obtained with *k-ω SST* model of turbulence with *ANSYS Fluent*. Horizontal cross-section at height z = 0.21 *m*; air velocity at inlet is 4.7 *m/s*

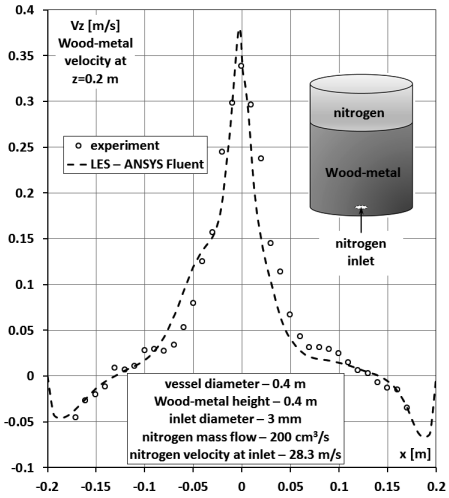

Figure 3. *Wood*-metal velocity vertical component for nitrogen–*Wood*-metal *CBR*. Comparison of experimental data [12] and computational results obtained with *LES* models of turbulence with *ANSYS Fluent*. Horizontal cross-section at height z = 0.2 *m*; nitrogen velocity at inlet is 28.3 *m/s*

• *CBR* with air (gas) and water (optically transparent and electrically non-conductive liquid without external magnetic) [8] – Figure 2;

• *CBR* with nitrogen (gas) and *Wood*-metal (optically non-transparent and electrically conductive liquid) [12] – Figure 3.

• *rectangle bubble reactor* (*RBR*) with air and water [13];

The predicted and measured profiles of vertical (axial) velocity of liquid are of a good qualitative and quantitative agreement.

RESULTS OF COMPUTATIONS

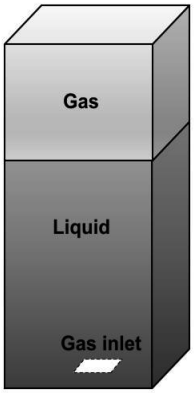

Figure 4. Scheme of computational model – *RBR* [13]

RBR (Figure 4) is chosen as the computational model. The geometry corresponds to [13]: vessel length and width are 0.5×0.2 *m*; water height – 1.5 m; inlet opening length and width are 0.18×0.08 *m*. Gas phase is air. Liquid phase has density of water, but the liquid is assigned electrically conductive ($\sigma_l^{EM} = 10^6\ \Omega^{-1} \cdot m^{-1}$). The reason is to keep the possibility to compare computational results with experimental data for optically transparent liquid.

Computational results are presented in Figures 5, 6. Note, that values of liquid volume fraction in gas zone above the liquid are extremely small, thus small values of liquid velocity can be neglected.

In the case of ***absence of magnetic field*** the jet of air has the instantaneous "snake-like" shape in the zone near inlet. In whole volume the flow is extremely chaotic – Figure 5 (left).

Time-averaged (flow time 20 s has been reached) distribution of air volume fraction is almost symmetrical to vertical plane – Figure 5 (right). Maximum time-averaged speed of liquid is $v_{l,max}^{aver} \sim 0.8$ *m/s*, which is ~1.6 times greater than gas speed in inlet opening $v_g^{inlet} = 0.5$ *m/s*. The instantaneous speed of liquid may exceed $v_{l,max}^{inst} \sim 1.65$ *m/s*.

In the case of the ***constant horizontal magnetic field***, the character of flow is less chaotic and air penetration into liquid is more expressed – Figure 6 (left). The instantaneous speed of liquid may exceed $v_{l,max}^{inst} \sim 1.95$ *m/s*. Maximum time-averaged speed of liquid is $v_{l,max}^{aver} \sim 1.33$ *m/s*, which is ~2.7 times greater than gas speed in inlet opening v_g^{inlet}.

In the case when the ***constant vertical magnetic field*** is applied, maximum time-averaged speed of liquid is $v_{l,max}^{aver} \sim 0.9$ *m/s*, which is ~1.8 times greater than gas speed in inlet opening v_g^{inlet}. The instantaneous speed of liquid may exceed $v_{l,max}^{inst} \sim 1.67$ *m/s*.

The liquid velocity is induced by bubble collective flow. When magnetic field is "switched on" the liquid velocity can exceed the greater values in comparison with the case without magnetic field. It can be explained with the following reasons:

• The flow of electrically conductive liquid in external magnetic field induces the EM force (Eq. 3). EM force breaks the vortices [14, p. 33], which are perpendicular to external magnetic field; the vortices, which are parallel to external magnetic field, are not affected with EM force (see scheme of vector fields in Figure 7). Note that in the case, when velocity vortex and magnetic field vectors are parallel, the electrical current is not induced (Figure 7, right, dotted lines) – there is not any source of current in the vortex and current lines are

closed ($div\ \vec{j}_l = 0$).

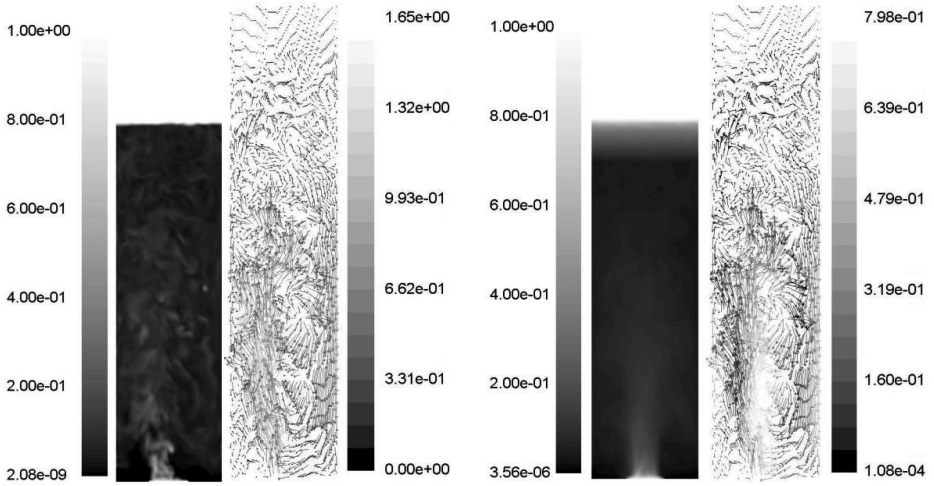

Figure 5. Rectangle bubble reactor. Magnetic field is "switched off" – $B = 0$. Instantaneous (flow time $t = 20$ *s*) (left) and averaged (flow time $t = 5$–20 *s*) (right) contours of gas volume fraction and velocity vectors of electrically conductive liquid (cross-sections $y = 0$) obtained with *LES* model of turbulence. Gas velocity at inlet is 0.5 *m/s* (gas mass flow $8.5 \cdot 10^{-3}$ *kg/s*).

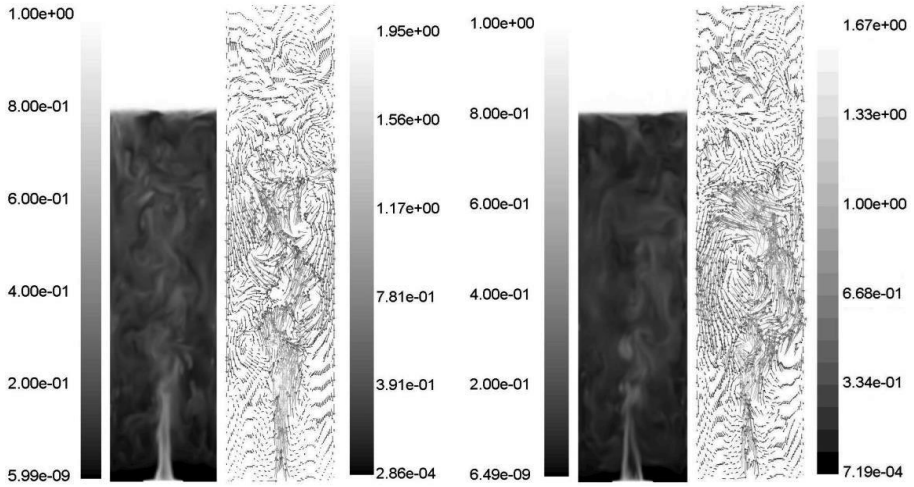

Figure 6. Rectangle bubble reactor. Horizontal B_x=0.1 *T* (left) and vertical B_z=0.1 *T* (right) magnetic field is "switched on" –vector of magnetic induction is parallel to the plane of figure. Instantaneous (flow time $t = 20$ *s*) contours of gas volume fraction and velocity vectors of electrically conductive liquid (cross-sections $y = 0$) obtained with *LES* model of turbulence. Gas velocity at inlet is 0.5 *m/s* (gas mass flow $8.5 \cdot 10^{-3}$ *kg/s*).

Due to incompressibility of liquid ($div\ \vec{v}_l = 0$) the mentioned effect of turbulent vortices breaking by EM force influence the spatial distribution of velocity.

• As vortices are slowing down by EM force, the turbulent resistance, acting to bubbles is smaller. This is the reason why the collective flow of bubbles can accelerate if compare with bubble flow without magnetic field.

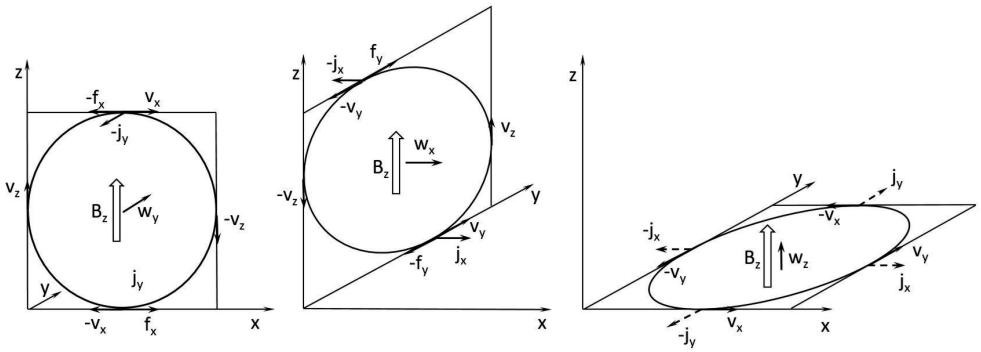

Figure 7. The scheme of vector fields in turbulent flow of electrically conductive liquid: liquid velocity is $\overrightarrow{\mathrm{v}_l} = \{\mathrm{v_x}, \mathrm{v_y}, \mathrm{v_z}\}$; liquid velocity vortex is $\vec{w}_l = \{w_\mathrm{x}, w_\mathrm{y}, w_\mathrm{z}\}$; induction of external magnetic field is $\overrightarrow{B_0} = \{0,0,B_\mathrm{z}\}$; induced electrical current in liquid is $\vec{j}_l = \{j_\mathrm{x}, j_\mathrm{y}, j_\mathrm{z}\}$; EM force in liquid is $\overrightarrow{f_l} = \{f_\mathrm{x}, f_\mathrm{y}, f_\mathrm{z}\}$.

CONCLUSIONS

√ In order to study the gas bubbles collective dynamics interfacing with the electrically conductive liquid flow in the bubble reactor, the numerical approach is developed, which is based on *Euler-Euler* multi-phase tools of commercial package *ANSYS Fluent with Magnetohydrodynamic module* with application of *k-ω Shear Stress Transport* and/or *Large Eddy Simulation* models of turbulence.

√ Computational results for the gas and liquid volume fractions and the velocity vectors in bubble reactor without magnetic field are of a good qualitative and quantitative agreement with the experimental and predicted results for the air–water two phase system in the rectangular and cylindrical bubble reactors as well for the nitrogen–*Wood*-metal cylindrical bubble reactor.

√ The constant magnetic field is regularizing the gas flow in reactor and makes it less chaotic. The gas and liquid flows are accelerated in external magnetic field due to breaking effect of electromagnetic force, which acts to turbulent vortices, and consequently makes smaller the turbulent resistance for bubble flow.

ACKNOWLEDGMENT

The current research is supported by the Helmholtz Association of German Research Centers, within the scope of the Helmholtz Alliance – Liquid Metal Technologies (LIMTECH).

REFERENCES

[1] Abánades, A., Ruiz, E., Ferruelo, E.M., Hernández, F., Cabanillas, A., Martínez-Val, J.M., Rubio, J.A., López, C., Gavela, R., Barrera, G., Rubbia, C., Salmieri, D., Rodilla, E., Gutiérrez, D. (2011). Experimental analysis of direct methane cracking. International

Journal on Hydrogen Energy, 36, 12877–12886.
[2] Hydrogen from methane without CO2 emissions (2013). Karlsruhe Institute of Technology, PR 041 (March 21).
[3] Steinberg, T., Baake, E. (2014). CO2-freie Produktion von Wasserstoff durch den Einsatz von Flüssigmetal. Elektrowärme International, 2, 59-62.
[4] Tucs, A., Spitans, S., Jakovics, A., Baake, E. (2013). Implementation and verification of numerical model for gas bubble dynamics in electroconductive fluid. Proceedings of AIP (American Institute of Physics) Conference, 1558, 86–89.
[5] Jakovics, A., Pavlovs, S., Baake, E., Steinberg, T., Sushkovs, V., Tatulcenkovs, A. (2015). Numerical study of gas bubbles collective dynamics in the melt influenced with magnetic field. Proceeding of the 8th International Conference on Electromagnetic Processing of Materials, 183–186.
[6] Multiphase flow theory (2011). In: ANSYS CFX-solver theory guide.
[7] Multiphase flows (2012). In: ANSYS Fluent theory guide.
[8] Lou, W., Zhu, M. (2013). Numerical simulation of gas and liquid two-phase flow in gas-stirred systems based on Euler–Euler approach. Metallurgical and Materials Transactions B, 44, 2013-1251.
[9] Spille-Kohoff, A. (2009). Arc welding: from process simulation to structural mechanics. Part I. Process simulation with ANSYS CFX. The 4th European Automotive Simulation Conference, 1–12.
[10] Trautmann, M., Hertel, M., Füssel, U., Spille-Kohoff, A. (2013). Magnetohydrodynamics and gas metal arc welding in ANSYS Fluent. ANSYS Conference & 31th CADFEM User's Metting, 1–21.
[11] Magnetohydrodynamic model theory (2013). In: ANSYS Fluent MHD module manual.
[12] Yongkun, X. (1991). Untersuchung der Strömung und des Blasenverhaltens in gasgerührten Wood-Metall-Schmelzen. Doktor-Ingenieur Dissertation. Berlin.
[13] Sanchez-Forero, D.I., Silva (Jr.), J.L., Silva, M.K., Bastos, J.C.S.C., Mori, M. (2013). Experimental and numerical investigation of gas-liquid flow in a rectangular bubble column with centralized aeration flow pattern. Chemical Engineering Transactions, 32, 1561–1566.
[14] Gelfgat, Yu.M., Lielausis, O.A., Shcherbinin, E.V. (1976). Liquid metal under the influence of electromagnetic forces. Riga (in Russian).